



Cite this: *RSC Adv.*, 2025, **15**, 15604

Received 29th March 2025  
 Accepted 29th April 2025

DOI: 10.1039/d5ra02189h  
[rsc.li/rsc-advances](http://rsc.li/rsc-advances)

## Optical and crystalline properties of benzo[1,2-*b*:4,5-*b'*]dithiophene derivatives†

Caiyun Guo, Yibin Wang, Chenghao Zhang, Hui Liu\* and Liangliang Han  \*

When designing solution-processable semiconducting molecules and polymers, benzo[1,2-*b*:4,5-*b'*]dithiophene (BDT) derivatives are widely used because of their planar structures, superior optical properties, ease of synthesis and ease of modification. In this work, four BDT derivatives—BDTT, BDTT-Et, BDTT-OMe and BDTT-CH<sub>2</sub>-OMe—were designed and synthesized with different side chains, considering the important roles of side chains in the performance of organic semiconductors. Especially for BDTT-CH<sub>2</sub>-OMe, with a new methoxymethyl chain, it exhibited excellent optical properties and the deepest highest occupied molecular orbital energy level ( $E_{HOMO}$ ) among these derivatives. Moreover, it demonstrated strong intermolecular interactions and tight  $\pi$ - $\pi$  stacking. The optical, electrochemical and crystalline properties suggested that BDTT-CH<sub>2</sub>-OMe could be further modified as a potential building block for the design of electron-donating small molecules (SMs) or polymers when used in organic electronics, such as bulk heterojunction organic solar cells (BHJ-OSCs).

## Introduction

Organic solar cells (OSCs) have emerged as a promising photovoltaic technique due to the advantages of low-cost fabrication, light weight, flexibility and compatibility with large-scale solution-processing technologies.<sup>1,2</sup> OSCs utilize various organic materials, offering unique advantages such as tunable optoelectronic properties and the prospect of environmentally friendly production processes.<sup>3–5</sup> Generally, there are four types of bulk heterojunction (BHJ) OSCs: polymeric donor with small molecule (SM) acceptor, polymeric donor with polymeric acceptor (all-polymer OSCs), SM donor with polymeric acceptor and SM donor with SM acceptor.<sup>6–8</sup> Regardless of the type of BHJ-OSCs, the design of optically active materials is highly critical. Ordinarily, the photophysical, electrochemical and electrical properties of the electron donors or acceptors are highly dependent on their physicochemical properties, such as molecular configuration, molecular weight, and packing patterns.<sup>9,10</sup>

Benzo[1,2-*b*:4,5-*b'*]dithiophene (BDT) is one of the most attractive electron-donating units and is a widely used chemical moiety for BHJ-OSCs. The BDT unit has a symmetric and planar conjugated structure, which leads to strong inter-molecular orbital overlap, improves the electron delocalization and  $\pi$ - $\pi$  stacking in thin solid films, and results in efficient charge

carrier transport in devices.<sup>11</sup> Moreover, the presence of a sulfur atom promotes the electron density *via* a lone electron pair, which increases the electron-donating capability of BDT. Furthermore, owing to their facile manufacturing procedures, BDT and its derivatives are primarily used as promising donors.<sup>12</sup>

To date, BDT has proven to be one of the most important fused-ring building blocks in the design of conjugated polymeric donors for BHJ-OSCs due to its high charge carrier mobility and deep-lying highest occupied molecular orbital energy level ( $E_{HOMO}$ ).<sup>13</sup> As an electron-donating moiety, BDT has been chosen for the following merits: (a) the fused BDT ring structure allows the incorporation of substituents on the central benzene core while maintaining the planarity of the two thiophene units; (b) its structural symmetry and the fused aromatic system enhance electron delocalization and inter-chain interactions, improving charge carrier mobility and eliminating the need to control regioregularity during the polymerization process; (c) it maintains a deep  $E_{HOMO}$  in the resulting polymers, as demonstrated by weak-donor and strong-acceptor polymers.<sup>14</sup> At the same time, BDT derivatives are widely used to construct SM electron donors or acceptors, ultimately forming an acceptor–donor–acceptor (A–D–A) structure. These SMs have rigid and planar skeletons that facilitate precise chemical customization, resulting in highly versatile molecular configurations, optical properties and electronic characteristics. Even subtle changes in molecular structure, such as modifications to side chains, end groups and  $\pi$  bridges, can have a significant impact on photovoltaic performance.<sup>15–17</sup>

Many side chains, such as alkyl chains, oxyalkyl chains and aromatic chains, have been introduced on the central benzene

College of Chemistry and Chemical Engineering, Yantai University, Yantai 264005, China. E-mail: [lh@ytu.edu.cn](mailto:lh@ytu.edu.cn); [hanll@ytu.edu.cn](mailto:hanll@ytu.edu.cn)

† Electronic supplementary information (ESI) available: TGA curves, NMR spectra, single-crystal X-ray analysis. CCDC 2411354, 2411365, 2411366 and 2417527. For ESI and crystallographic data in CIF or other electronic format see DOI: <https://doi.org/10.1039/d5ra02189h>



unit of BDT to optimize the optical, electrochemical and electrical characteristics of the solution processed semi-conducting polymers and SMs.<sup>18</sup> Moreover, the aromatic chain-substituted BDT (2D-BDT) strategy demonstrates unique advantages compared to other substituents, particularly when two thiophene rings are introduced. Note that the conjugated groups in the orthogonal direction of BDT can delocalize  $\pi$ -electrons to BDT, thereby increasing the  $\pi$  conjugation and UV-vis absorption. Moreover, these aromatic substituents can optimize the inter-chain  $\pi$ - $\pi$  stacking and energy levels of the final semi-conducting materials.<sup>19</sup>

In addition, the flexible side chains that ensure solubility have also been studied for organic electronics. These chains play a very important role in the optimization of bandgaps, optical properties and electrical characteristics. Therefore, significant attention has been given to the design and synthesis of BDT materials.<sup>20-22</sup> In this work, four BDT derivatives—4,8-di(thiophen-2-yl)benzo[1,2-*b*:4,5-*b'*]dithiophene (BDTT), 4,8-bis(5-ethylthiophen-2-yl)benzo[1,2-*b*:4,5-*b'*]dithiophene (BDTT-Et), 4,8-bis(5-methoxythiophen-2-yl)benzo[1,2-*b*:4,5-*b'*]dithiophene (BDTT-OMe) and 4,8-bis(5-(methoxymethyl)thiophen-2-yl)benzo[1,2-*b*:4,5-*b'*]dithiophene (BDTT-CH<sub>2</sub>-OMe)—were synthesized with the aim of revealing how different side chains influence the optical, electrochemical and stacking characteristics of BDT and providing fundamental insights into the design of semiconducting materials. The newly designed BDTT-CH<sub>2</sub>-OMe exhibited clear advantages and could be considered a potential building block for the construction of semiconducting polymers and SMs.

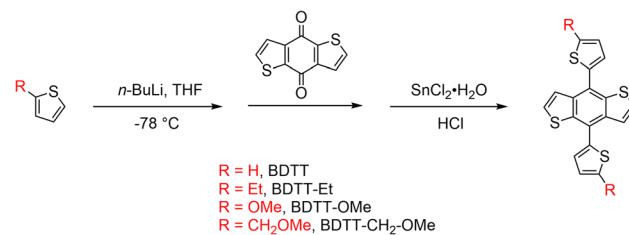
## Results and discussion

Alkyl and oxyalkyl chains are the most popular side chains that can provide favorable solubility; moreover, they optimize the crystallization of semiconductors too. However, the introduction of alkyl chains on thiophene always leads to poor production yields and a difficult purification process, especially when bulky or long alkyl chains are employed.<sup>23</sup> Oxyalkyl chain-substituted thiophene can be easily obtained, but the oxygen atom could remarkably increase the  $E_{HOMO}$  of the polymers or SMs owing to a strong p- $\pi$  conjugative effect, which is not conducive to obtain high open-circuit voltage ( $V_{OC}$ ) when the polymers are used as electron donors in OSCs.<sup>24</sup> Therefore, understanding the manner in which a thiophene with soluble chains can be achieved and how the influence of a strong conjugative effect on the conjugated backbone can be avoided has become very important. Here, a new alkoxyethyl chain was designed and synthesized in comparison with alkyl and oxyalkyl groups. To facilitate the growth of single crystals of the compounds, the alkyl, oxyalkyl and alkoxyethyl chains were represented by ethyl, methoxyl and methoxymethyl groups, respectively. All compounds were synthesized as per previously reported procedures.<sup>25</sup> Benzo[1,2-*b*:4,5-*b'*]dithiophene-4,8-dione was used as the starting material, treated with different thiophene lithium salts, and then reduced in the presence of SnCl<sub>2</sub>·2H<sub>2</sub>O in a 10% HCl solution. BDTT-Et, BDTT-OMe and BDTT-CH<sub>2</sub>-OMe, with different types of side chains, were

designed to investigate their optical, electrochemical and crystal properties, while BDTT was used as a reference molecule (Scheme 1).

## Optical properties

The UV-vis absorption and photoluminescence (PL) spectra of BDTT, BDTT-Et, BDTT-OMe and BDTT-CH<sub>2</sub>-OMe in chloroform solutions are shown in Fig. 1a and c, respectively. A distinctive redshifted transition was observed for BDTT-OMe (Table 1), which was mainly due to the electron-donating p- $\pi$  conjugation effect of the oxygen atom. This result agreed well with previous reports.<sup>26</sup> To eliminate the effect of solvation, we also tested the UV-vis absorption and PL spectra of these four BDT derivatives in toluene, tetrahydrofuran and ethanol solutions, which showed the same trend as in chloroform solution (Fig. S1†). BDTT-Et and BDTT-CH<sub>2</sub>-OMe showed slight redshifted transitions compared to BDTT, indicating that the electron-donating  $\sigma$ - $\pi$  hyperconjugation effects of the alkyl chains existed, or that the presence of side chains might influence the molecular configuration of BDTT. It should be noted that these characteristics are independent of molecular aggregation in dilute chloroform solutions. However, in their thin film states, the shape of the PL spectra for BDTT-OMe and BDTT-CH<sub>2</sub>-OMe (Fig. 1d) exhibited distinctive shoulder peaks compared to BDTT and BDTT-Et. This suggested that the oxygen atom played an important role in the aggregation of BDTT. Many studies have shown that oxygen atoms can increase intra-molecular/inter-molecular interactions through weak O···H or O···S interactions, thereby optimizing the planarity and stacking properties of the polymers.<sup>27,28</sup> This enhanced inter-molecular interaction may explain the change in the solid-state PL peak patterns of BDTT-OMe and BDTT-CH<sub>2</sub>-OMe.<sup>29</sup> All the molecules had high molar extinction coefficients ( $\epsilon$ ) of  $10.26 \times 10^5$ ,  $8.51 \times 10^5$ ,  $9.41 \times 10^5$  and  $10.16 \times 10^5$  L mol<sup>-1</sup> cm<sup>-1</sup> for BDTT, BDTT-Et, BDTT-OMe and BDTT-CH<sub>2</sub>-OMe, respectively, measured in their chloroform solutions (Fig. 1b). The light absorption efficiency directly affects the ability of the material to capture incident light. The  $\epsilon$  of BDTT-CH<sub>2</sub>-OMe was higher than that of the ethyl and methoxyl substituted molecules, which was crucial when considering its application in OSCs. The differences in optical properties for BDTT derivatives indicated that the introduction of side chains might have an impact on their molecular aggregation and crystallinity. At the same time, the electronic effects of side chains are also crucial,



Scheme 1 Synthetic method for BDTT, BDTT-Et, BDTT-OMe and BDTT-CH<sub>2</sub>-OMe.



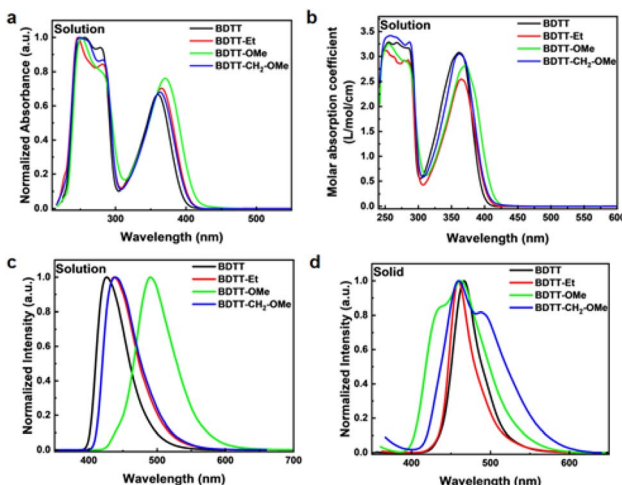


Fig. 1 (a) Normalized UV-vis absorption spectra of the four compounds in chloroform solution at a concentration of  $1 \times 10^{-5}$  mol L<sup>-1</sup>. (b) Molar absorption coefficients of the four compounds. (c) PL spectra of the four compounds in chloroform solution at a concentration of  $1 \times 10^{-5}$  mol L<sup>-1</sup>. (d) PL spectra of the four compounds in their solid states.

Table 1 UV-vis absorption, PL and electrochemical data of BDTT, BDTT-Et, BDTT-OMe and BDTT-CH<sub>2</sub>-OMe

Compound	$E_g^{\text{opt}}$ [eV]	$E_{\text{ox}}$ [V]	$E_{\text{red}}$ [V]	$E_{\text{HOMO}}$ [eV]	$E_{\text{LOMO}}$ [eV]
BDTT	1.86	1.08	-0.78	-5.43	-3.57
BDTT-Et	1.74	0.99	-0.75	-5.34	-3.60
BDTT-OMe	1.38	0.70	-0.68	-5.05	-3.67
BDTT-CH <sub>2</sub> -OMe	1.88	1.13	-0.77	-5.48	-3.60

making the choice of side chains more complicated and worthy for further exploration.

### Electrochemical properties

The electrochemical properties of these molecules are studied using cyclic voltammetry (CV) and are shown in Fig. 2a. The energy level diagrams of these molecules are shown in Fig. 2b. BDTT-Et and BDTT-OMe have predictably lower oxidation

potentials ( $E_{\text{ox}}$ ) than BDTT (Table 1); however, interestingly, BDTT-CH<sub>2</sub>-OMe has a considerably higher  $E_{\text{ox}}$  compared to other derivatives, a reasonable explanation for this is that the methoxymethyl group exhibits a very weak electron donating effect and even shows a weak electron withdrawing effect because of the higher  $E_{\text{ox}}$  and decreased  $E_{\text{HOMO}}$  compared with BDTT. The separation of oxygen atom and thiophene ring by the insertion of a methylene does achieve the idea of how to design a BDT derivative that can maintain low  $E_{\text{HOMO}}$  to compensate for the insufficiency of the alkyl chains. Electrochemical data provide additional evidence for the potential application of BDTT-CH<sub>2</sub>-OMe on the design of electron donors for OSCs.

### X-ray diffraction

Finally, the crystal structures were studied to understand the influence of different side chains on the packing patterns of BDTT derivatives. X-ray single-crystal diffraction showed that BDTT formed an orthorhombic crystal structure with a specific molecular arrangement and symmetry.<sup>30,31</sup> In contrast, BDTT-Et, BDTT-OMe and BDTT-CH<sub>2</sub>-OMe adopted monoclinic crystal structures with  $\beta$  angles of 101.118°, 104.263° and 104.165°, respectively, indicating that the introduction of substituents increased steric hindrance and disrupted orthorhombic symmetry. The dihedral angles between the side thiophene ring and the central BDT unit were 45.17°, 59.63° and 44.75° for BDTT-Et, BDTT-OMe and BDTT-CH<sub>2</sub>-OMe, respectively, all larger than that of BDTT (35.86°). However, the  $\pi$ - $\pi$  stacking distances ( $d_{\pi}$ ), calculated from the diffraction data, indicated that BDTT-Et, BDTT-OMe and BDTT-CH<sub>2</sub>-OMe exhibited tighter packing than BDTT (Fig. 3), with BDTT-CH<sub>2</sub>-OMe showing the smallest  $d_{\pi}$  value. The  $d_{\pi}$  values for BDTT, BDTT-Et, BDTT-OMe and BDTT-CH<sub>2</sub>-OMe were 3.693 Å, 3.579 Å, 3.472 Å and 3.392 Å, respectively. These results demonstrated that flexible side chains had minimal influence on the  $\pi$ - $\pi$  stacking of BDTT; moreover, they could promote tighter packing of adjacent molecules. In BHJ-OSCs, controlling the  $d_{\pi}$  can significantly affect the charge transfer performance of the materials. Reducing the  $d_{\pi}$  distance enhances charge transfer between adjacent molecules, thereby improving carrier mobility and photovoltaic performance. For example, silicon-based substitution<sup>20</sup> has proven to be an effective strategy for designing high-performance conjugated polymers or SMs. The

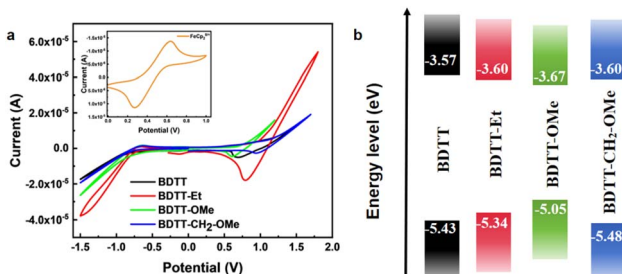


Fig. 2 (a) CV curves of the four compounds in a 0.1 mol per L acetonitrile solution, scan rate: 20 mV s<sup>-1</sup>, with ferrocene/ferrocenium (Fc/Fc<sup>+</sup>) couple provided as internal standard. (b) Energy level diagrams of the four compounds.

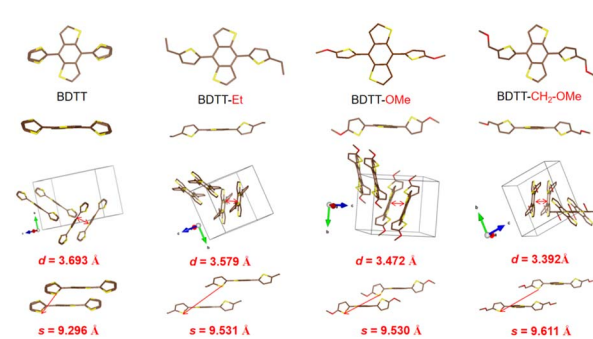


Fig. 3 Crystal structures of BDTT, BDTT-Et, BDTT-OMe and BDTT-CH<sub>2</sub>-OMe.



distances between sulfur atoms on any two parallel thiophene side chains in BDTT, BDTT-Et, BDTT-OMe and BDTT-CH<sub>2</sub>-OMe were 9.269 Å, 9.531 Å, 9.530 Å and 9.611 Å, respectively. This trend aligns well with previously reported results, as the distance is generally proportional to the length of the side chain.<sup>32</sup> BDTT exhibited the shortest distance, while BDTT-CH<sub>2</sub>-OMe showed the longest, consistent with the methoxymethyl group being the longest chain among them. The X-ray single-crystal diffraction data also highlighted BDTT-CH<sub>2</sub>-OMe as a potential building block for the design of semiconductors with tight  $\pi$ - $\pi$  stacking, which was beneficial for charge carrier transport.<sup>28</sup>

Although the optical, electrochemical properties and crystal structure of the monomer do not directly correspond to the photovoltaic properties of the final polymer, many studies have shown that investigating the fundamental physical and chemical properties of the monomer can help explain the photoelectric properties of the resulting polymer.<sup>28,30,31,33</sup> We believe that the lower  $E_{\text{HOMO}}$  and tighter  $\pi$ - $\pi$  stacking of BDTT-CH<sub>2</sub>-OMe likely influence the photoelectric properties of the polymer. In particular, the low  $E_{\text{HOMO}}$  is highly favorable for achieving a high open-circuit voltage. The design and performance characterization of polymers based on BDTT-CH<sub>2</sub>-OMe are currently in progress in our laboratory. In addition, thermogravimetry analysis of the different derivatives (Fig. S2†) showed that BDTT-CH<sub>2</sub>-OMe exhibited excellent thermal stability, with a thermal decomposition temperature exceeding 200 °C, which met the requirements for solar cell materials.

## Conclusions

In summary, four BDT derivatives—BDTT, BDTT-Et, BDTT-OMe and BDTT-CH<sub>2</sub>-OMe—were designed and synthesized with different thiophene side chains. The photophysical, electrochemical and crystallographic properties were also characterized to assess the potential application of these molecules in the design of semiconducting polymers and SMs. Among these, the newly designed BDTT-CH<sub>2</sub>-OMe exhibited excellent packing patterns and a deeper  $E_{\text{HOMO}}$  of -5.48 eV compared to the other derivatives, making it particularly beneficial for the design of electron donors in BHJ-OSCs. These results indicated that the methoxymethyl side chain can not only function as a flexible side chain to improve the solubility of the final semiconducting materials, similar to alkyl chains, but also enhance intermolecular interactions due to the introduction of the oxygen atom. At the same time, it disrupts the strong  $\pi$ - $\pi$  conjugation effect, making BDTT-CH<sub>2</sub>-OMe a potential candidate for designing semiconducting materials. BDTT-CH<sub>2</sub>-OMe exhibited similar absorption to other analogues but showed an obvious red-shift in PL, caused by strong intermolecular interactions. Although BDTT-CH<sub>2</sub>-OMe had relative lower stability, this limitation could be addressed through chemical design and modification.

## Data availability

Supplementary crystallographic data for BDTT, BDTT-Et, BDTT-OMe and BDTT-CH<sub>2</sub>-OMe have been deposited at the

CCDC under deposition numbers 2411354, 2411365, 2417527 and 2411366.

## Conflicts of interest

There are no conflicts to declare.

## Acknowledgements

This work was supported by the National Natural Science Foundation of China (51873227), the Shandong Provincial Natural Science Foundation (ZR2015EQ002) and the Qingdao Applied and Fundamental Research (16-5-1-94-jch).

## Notes and references

- 1 B. Ma, Y. Yan, M. Wu, S. Li, M. Ru, Z. Xu and W. Zhao, *Adv. Funct. Mater.*, 2024, **35**, 2413814.
- 2 Y. Yan, B. Duan, M. Ru, Q. Gu, S. Li and W. Zhao, *Adv. Energy Mater.*, 2024, **15**, 2404233.
- 3 R. Yu, H. Yao, Z. Chen, J. Xin, L. Hong, Y. Xu, Y. Zu, W. Ma and J. Hou, *Adv. Mater.*, 2019, **31**, 477–485.
- 4 C. Xiao, X. Wang, T. Zhong, R. Zhou, X. Zheng, Y. Liu, T. Hu, Y. Luo, F. Sun, B. Xiao, Z. Liu, C. Yang and R. Yang, *Adv. Sci.*, 2023, **10**, 2206580.
- 5 X. Kong, J. Zhang, L. Meng, C. Sun, X. Jiang, J. Zhang, C. Zhu, G. Sun, J. Li, X. Li, Z. Wei and Y. Li, *CCS Chem.*, 2023, **5**, 2945–2955.
- 6 Z. Zhang, Y. Wang, C. Sun, Z. Liu, H. Wang, L. Xue and Z. Zhang, *Nano Sel.*, 2021, **3**, 233–247.
- 7 F. Langa, P. de la Cruz and G. D. Sharma, *ChemSusChem*, 2024, **18**, 361–413.
- 8 W. Peng, J. Xiong, T. Chen, D. Zhao, J. Liu, N. Zhang, Y. Teng, J. Yu and W. Zhu, *RSC Adv.*, 2024, **14**, 8081–8089.
- 9 X. Li, I. Angunawela, Y. Chang, J. Zhou, H. Huang, L. Zhong, A. Liebman-Pelaez, C. Zhu, L. Meng, Z. Xie, H. Ade, H. Yan and Y. Li, *Energy Environ. Sci.*, 2020, **13**, 5028–5038.
- 10 A. Venkatalaxmi, B. S. Padmavathi and T. Amaranath, *Fluid Dyn. Res.*, 2004, **35**, 229–236.
- 11 X. Yin, Q. An, J. Yu, Z. Xu, P. Deng, Y. Geng, B. Zhou, F. Zhang and W. Tang, *Dyes Pigm.*, 2017, **140**, 512–519.
- 12 H. Yao, L. Ye, H. Zhang, S. Li, S. Zhang and J. Hou, *Chem. Rev.*, 2016, **116**, 7397–7457.
- 13 Y. Lin, Y. Li and X. Zhan, *Chem. Soc. Rev.*, 2012, **41**, 4245–4272.
- 14 K. Lai, C. Chang and C. W. Chu, *Org. Electron.*, 2021, **89**, 106010.
- 15 Z. Luo, T. Liu, W. Cheng, K. Wu, D. Xie, L. Huo, Y. Sun and C. Yang, *J. Mater. Chem. C*, 2018, **6**, 1136–1142.
- 16 Q. V. Hoang, C. E. Song, I.-N. Kang, S.-J. Moon, S. K. Lee, J.-C. Lee and W. S. Shin, *RSC Adv.*, 2016, **6**, 28658–28665.
- 17 J. Li, M. Lin, H. Wang, J. Iqbal and K. Wang, *Dyes Pigm.*, 2025, **233**, 112508–112515.
- 18 J. Zhou, Y. Zuo, X. Wan, G. Long, Q. Zhang, W. Ni, Y. Liu, Z. Li, G. He, C. Li, B. Kan, M. Li and Y. Chen, *J. Am. Chem. Soc.*, 2013, **135**, 8484–8487.



19 M. Li, W. Ni, X. Wan, Q. Zhang, B. Kan and Y. Chen, *J. Mater. Chem. A*, 2015, **3**, 4765–4776.

20 H. Bin, L. Gao, Z. Zhang, Y. Yang, Y. Zhang, C. Zhang, S. Chen, L. Xue, C. Yang, M. Xiao and Y. Li, *Nat. Commun.*, 2016, **7**, 13651–13659.

21 Y. Qin, H. Chen, J. Yao, Y. Zhou, Y. Cho, Y. Zhu, B. Qiu, C.-W. Ju, Z.-G. Zhang, F. He, C. Yang, Y. Li and D. Zhao, *Nat. Commun.*, 2020, **11**, 5814–5824.

22 J. Wu, G. Li, J. Fang, X. Guo, L. Zhu, B. Guo, Y. Wang, G. Zhang, L. Arunagiri, F. Liu, H. Yan, M. Zhang and Y. Li, *Nat. Commun.*, 2020, **11**, 4612–4619.

23 X. Yin, Q. An, J. Yu, F. Guo, Y. Geng, L. Bian, Z. Xu, B. Zhou, L. Xie, F. Zhang and W. Tang, *Sci. Rep.*, 2016, **6**, 25355–25361.

24 X. Wang, J. Wang, J. Han, D. Huang, P. Wang, L. Zhou, C. Yang, X. Bao and R. Yang, *Nano Energy*, 2021, **81**, 31185–31194.

25 E. Zhu, G. Ge, J. Shu, M. Yi, L. Bian, J. Hai, J. Yu, Y. Liu, J. Zhou and W. Tang, *J. Mater. Chem. A*, 2014, **2**, 13580–13586.

26 Q. Zhang, Y. Wang, B. Kan, X. Wan, F. Liu, W. Ni, H. Feng, T. P. Russell and Y. Chen, *Chem. Commun.*, 2015, **51**, 15268–15271.

27 T. L. Nguyen, H. Choi, S. J. Ko, M. A. Uddin, B. Walker, S. Yum, J. E. Jeong, M. H. Yun, T. J. Shin, S. Hwang, J. Y. Kim and H. Y. Woo, *Energy Environ. Sci.*, 2014, **7**, 3040–3051.

28 I. Osaka, M. Shimawaki, H. Mori, I. Doi, E. Miyazaki, T. Koganezawa and K. Takimiya, *J. Am. Chem. Soc.*, 2012, **134**, 3498–3507.

29 P. Yin, Q. Wan, Y. Niu, Q. Peng, Z. Wang, Y. Li, A. Qin, Z. Shuai and B. Tang, *Adv. Electron. Mater.*, 2020, **6**, 2000255.

30 A. C. Stuart, J. R. Tumbleston, H. Zhou, W. Li, S. Liu, H. Ade and W. You, *J. Am. Chem. Soc.*, 2013, **135**, 1806–1815.

31 C. B. Nielsen, A. J. P. White and I. McCulloch, *J. Org. Chem.*, 2015, **80**, 5045–5048.

32 P. Zhan, W. Zhang, I. E. Jacobs, D. M. Nisson, R. Xie, A. R. Weissen, R. H. Colby, A. J. Moulé, S. T. Milner, J. K. Maranas and E. D. Gomez, *J. Polym. Sci., Part B: Polym. Phys.*, 2018, **56**, 1193–1202.

33 L. Han, H. Jiang, D. Ouyang, W. Chen, T. Hu, J. Wang, S. Wen, M. Sun and R. Yang, *Nano Energy*, 2017, **36**, 110–117.

